Article ID:0253-2778(2016)06-0462-08

η transition form factor: A combined analysis of space- and time-like experimental data through rational approximants

ESCRIBANO R.[1,2]

(1. *Departament de Física, Universitat Autònoma de Barcelona, Grup de Física Teòrica E*-08193 *Bellaterra, Spain*;
2. *Institut de Física d'Altes Energies, The Barcelona Institute of Science and Technology, Campus UAB, E*-08193 *Bellaterra, Spain*)

Abstract: A combined analysis of the space- and time-like experimental data for the η transition form factor is performed in a model-independent way by means of rational approximants. The recent measurement of the e^+e^- invariant mass spectrum of the $\eta \to e^+e^-\gamma$ decay provided by the A2 Collaboration allowed us to extract the most precise and up-to-date slope and curvature parameters of the form factor. The impact of this new analysis on the η-η' mixing parameters and the $VP\gamma$ couplings is also discussed.

Key words: η transition form factor; space- and time-like data analysis; rational approximants; slope and curvature parameters; η-η' mixing; $V \to P\gamma$ radiative decays

CLC number: O572.3 **Document code**: A doi:10.3969/j.issn.0253-2778.2016.06.003

Citation: Escribano R. η transition form factor: A combined analysis of space- and time-like experimental data through rational approximants[J]. Journal of University of Science and Technology of China, 2016,46(6):462-469.
Escribano R. η 跃迁形状因子:合理近似的类时和类空实验数据的综合分析[J]. 中国科学技术大学学报,2016,46(6): 462-469.

η 跃迁形状因子:合理近似的类时和类空实验数据的综合分析

ESCRIBANO R.[1,2]

(1. 巴塞罗那自治大学,E-08193,西班牙;2. 巴塞罗那科学与技术研究所,E-08193,西班牙)

摘要:通过合理的近似,用类时和类空实验数据对 η 的跃迁形状因子进行了模型无关的综合分析. 最近 A2 合作组提供的衰变道不变质量谱的测量使我们能够提取最新、最精确的形状因子斜率和曲率参数, 并讨论了新分析对混合参数的影响和 $VP\gamma$ 耦合.

关键词:η 跃迁形状因子; 类时和类空数据分析;合理近似; 斜率和曲率参数; 合 辐射衰变

0 Introduction

The pseudoscalar transition form factors (TFFs) describe the effect of the strong interaction on the $\gamma^*\gamma^*P$ vertex, where $P = \pi^0, \eta, \eta', \eta_c \cdots$, and is represented by $F_{P\gamma^*\gamma^*}(q_1^2, q_2^2)$, a function of the

Received:2015-11-30;**Revised**:2016-04-20

Foundation item: Supported in part by the the Ministerio de Ciencia e Innovación (FPA2011-25948), the Ministerio de Economía y Competitividad (CICYT-FEDER-FPA 2014-55613-P, SEV-2012-0234), the Secretaria d´Universitats i Recerca del Departament d'Economia i Coneixement de la Generalitat de Catalunya(2014 SGR 1450), the Spanish Consolider-Ingenio 2010 Programme CPAN(CSD2007-00042).

Biography: Escribano R(corresponding author), Professor/PhD. Research field: high energy physics. E-mail: rafel.escribano@ifae.es

photon virtualities q_1^2, and q_2^2. From the experimental point of view, one can study such TFFs from both space- and time-like energy regions. The time-like region of the TFF can be accessed at meson facilities either through the double Dalitz decay processes $P\to l^+l^-l^+l^-$, which give access to both photon virtualities (q_1^2, q_2^2) in the range $4m_l^2 < (q_1^2, q_2^2) < (m_P - 2m_l)^2$, or the single Dalitz decay processes $P\to l^+l^-\gamma$, which contains a single virtual photon with transferred momentum in the range $4m_l^2 < q_1^2 < m_P^2$, thus simplifying the TFF to $F_{P\gamma^*\gamma^*}(q_1^2, 0) \equiv F_{P\gamma^*\gamma^*}(q^2)$. To complete the time-like region, e^+e^- colliders access to the values $q^2 > m_P^2$ through the $e^+e^-\to P\gamma$ annihilation processes. The space-like region of the TFFs are accessed in e^+e^- colliders by the two-photon-fusion reaction $e^+e^-\to e^+e^-P$, where at the moment the measurement of both virtualities is still an experimental challenge. The common practice is then to extract the TFF when one of the outgoing leptons is tagged and the other is not, that is, the single-tag method. The tagged lepton emits a highly off-shell photon with transferred momentum $q_1^2 \equiv -Q^2$ and is detected, while the other, untagged, is scattered at a small angle with $q^2 \simeq 0$. The form factor extracted from the single-tag experiment is then $F_{P\gamma^*\gamma^*}(-Q^2, 0) \equiv F_{P\gamma^*\gamma}(Q^2)$.

At low-momentum transfer, the TFF can be described by the expansion

$$F_{P\gamma^*\gamma}(Q^2) = F_{P\gamma\gamma}(0)\left(1 - b_P\frac{Q^2}{m_P^2} + c_P\frac{Q^4}{m_P^4} + \cdots\right) \quad (1)$$

where $F_{P\gamma\gamma}(0)$ is the normalization, the low-energy parameters (LEPs) b_P and c_P are the slope and the curvature of the TFF, respectively, and m_P is the pseudoscalar meson mass. $F_{P\gamma\gamma}(0)$ can be obtained either from the measured two-photon partial width of the meson P or, in the case of π^0, η and η', from the prediction of the axial anomaly in the chiral limit of QCD.

The slope parameter has been extensively discussed from both theoretical analyses[1-5] and experimental measurements[6-12]. With respect to the experimental determinations, the values for the slope are usually obtained after a fit to data using a normalized, single-pole term with an associated mass Λ_P, i. e.

$$F_{P\gamma^*\gamma}(Q^2) = \frac{F_{P\gamma\gamma}(0)}{1 + Q^2/\Lambda_P^2} \quad (2)$$

The A2 Collaboration reported $b_\eta = 0.59(5)$ [12], the most precise experimental determination up to date. The curvature was for the first time reported in Ref. [3] with the value $c_\eta = 0.37(10)_{\text{stat}}(7)_{\text{sys}}$.

Several attempts to describe the η TFF are available in the literature at present[2, 4-5, 13-27] but none of them tries for a unique description of both space- and time-like experimental data, specially at low energies. In Ref. [28], it was suggested for the π^0 case that a model-independent approach to the space-like TFF can be achieved using a sequence of rational functions, the Padé approximants (PAs), to fit the data. Later on, in Ref. [3], the same method was applied to the η and η' TFFs. More recently, the A2 Collaboration reported a new measurement of the $\eta\to e^+e^-\gamma$ Dalitz decay process with the best statistical accuracy up to date[12]. A comparison with different theoretical approaches was also performed. In particular, the results from Ref. [3], based on space-like data, were extrapolated to the time-like region and agreed perfectly with their measurement. Triggered by these new A2 results, we explore in the present work a combined description of both space- and time-like regions of the η TFF within our method of rational approximants. This will provide, for the first time, a determination of the energy dependence of the η TFF in both regions together with a unified extraction of its LEPs.

Our approach makes use of PAs as fitting functions to all the experimental data. PAs are rational functions $P_M^N(Q^2)$ (ratio of a polynomial $T_N(Q^2)$ of order N and a polynomial $R_M(Q^2)$ of order M) constructed in such a way that they have the same Taylor expansion as the function to be approximated up to order $\mathcal{O}(Q^2)^{N+M+1}$ [29]. Since PAs are built in our case from the unknown low-energy parameters (LEPs) of the TFF, once the fit to the experimental data is done, the reexpansion of the PAs yields the desired

coefficients. The advantage of PAs over Taylor expansions is their ability to enlarge the domain of convergence. However, to prove the convergence of a given PA sequence is a difficult task and only for certain classes of functions can this be done rigorously. In practice, the success of PAs in the description of experimental data can only be seen a posteriori in the sense that the pattern of convergence can be shown but unfortunately not proven mathematically. We refer the interested reader to Refs. [30-31] for details on this technique.

1 η transition form factor: a space- and time-like description

To extract the η TFF low-energy parameters b_η and c_η (slope and curvature, respectively) from the available data, we start with a $P_1^L(Q^2)$ sequence. However, according to Ref. [32], the pseudoscalar TFFs behave as $1/Q^2$ for $Q^2 \to \infty$, which means that, for any value of L, one will obtain in principle a good fit only up to a finite value of Q^2 but not for $Q^2 \to \infty$. Therefore, it would be desirable to incorporate this asymptotic-limit information in the fits to $Q^2 F_{\eta\gamma^*\gamma}(Q^2)$ by considering also a $P_N^N(Q^2)$ sequence.

Experimental data from the space-like region is obtained from CELLO, CLEO, and BABAR Collaborations[7-8, 33], together with the time-like experimental data from NA60 and A2 Collaborations[9-10, 12]. We also include the value $\Gamma_{\eta\to\gamma\gamma} = 0.516(18)$ keV[34] (which is basically dominated by the recent KLOE-2 measurement[35]) in our fits.

We start fitting with a $P_1^L(Q^2)$ sequence. We reach $L = 7$, shown in Fig. 1 as a green-dashed line. The smaller plot in Fig. 1 is a zoom into the time-like region. The obtained LEPs are shown in Fig. 2 together with our previous results (empty orange) when only space-like data were included in our fits[3]. The stability observed for the LEPs with the $P_1^L(Q^2)$ sequence is remarkable, and the impact of the inclusion of time-like data is clear since it not only allows us to reach higher precision on each PA but also to enlarge our PA sequence by 2 elements. The stability of the result is also clearer and reached earlier, reduces our systematic error, and shows the ability of our method to extract, for the first time, the LEPs from a combined fit to all the available data.

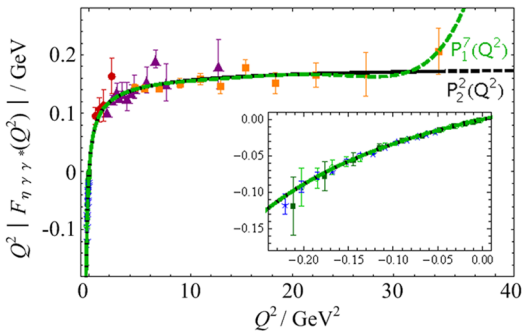

Fig. 1 η-TFF best fits

In Fig. 1, The gray-dashed line shows our best $P_1^L(Q^2)$ fit and the black line our best $P_N^N(Q^2)$ fit. Experimental data points in the space-like region are from CELLO (circles)[7], CLEO (triangles)[8], and BABAR (squares)[33] Collaborations. Experimental data points in the time-like region are from NA60 (stars)[9], A2 2011 (dark squares)[10], and A2 2013 (empty circles)[12]. The inner plot shows a zoom into the time-like region.

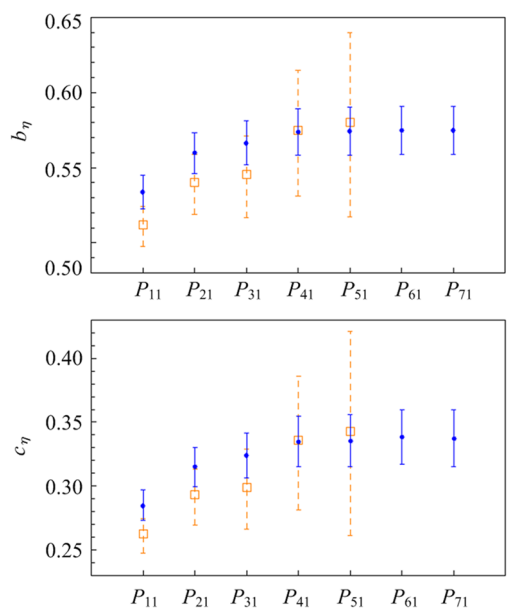

Fig. 2 Slope and curvature predictions for the η TFF using the $P_1^L(Q^2)$ up to $L = 7$ (solid line)

Previous results considering only space-like data

from Ref. [3] are also shown (empty squares) as a way to stress the role of the time-like data in our fits. Only statistical errors are shown.

To reproduce the asymptotic behavior of the TFF, we have also considered the $P_N^N(Q^2)$ sequence. The results obtained are in very nice agreement with our previous determinations. The best fit is shown by the black-solid line in Fig. 1. We reach $N=2$. Since these approximants contain the correct high-energy behavior built-in, they can be extrapolated up to infinity (black-dashed line in Fig. 1) and then predict the leading $1/Q^2$ coefficient:

$$\lim_{Q^2\to\infty} Q^2 F_{\eta\gamma^*\gamma}(Q^2) = 0.177^{+0.020}_{-0.009}\ \text{GeV} \qquad (3)$$

This prediction, although larger than in our previous work[3], still cannot be satisfactorily compared with the BABAR time-like measurement at $q^2 = 112\ \text{GeV}^2$, $F_{\eta\gamma^*\gamma}(112\ GeV^2) = 0.229(30)(8)\ \text{GeV}$[36]. The impact of such discrepancy in the η-η' mixing is discussed in the next section.

Our combined weighted average results, taking into account both types of PA sequences, give

$$\left.\begin{aligned} b_\eta &= 0.576(11)_{\text{stat}}(4)_{\text{sys}} \\ c_\eta &= 0.339(15)_{\text{stat}}(5)_{\text{sys}} \end{aligned}\right\} \qquad (4)$$

where the second error is systematic (around 0.7 and 1.5% for b_P and c_P, respectively.

Eq. (4) can be compared with $b_\eta = 0.60(6)_{\text{stat}}(3)_{\text{sys}}$ and $c_\eta = 0.37(10)_{\text{stat}}(7)_{\text{sys}}$ using space-like data exclusively[3]. As expected, not only statistical results have been improved but also systematics, both by an order of magnitude, yielding the most precise slope determination ever.

Our slope is compared with experimental determinations from Refs. [6-12] together with theoretical extraction from Refs. [1-5, 37-38] in Fig. 3.

One should notice that all the previous collaborations used a VMD model fit to extract the slope. In order to be consistent when compared with our results, a systematic error of about 40% should be added to the experimental determinations based on space-like data[3, 28], and a systematic error of about 5% should be added to the experimental determinations based on time-like data.

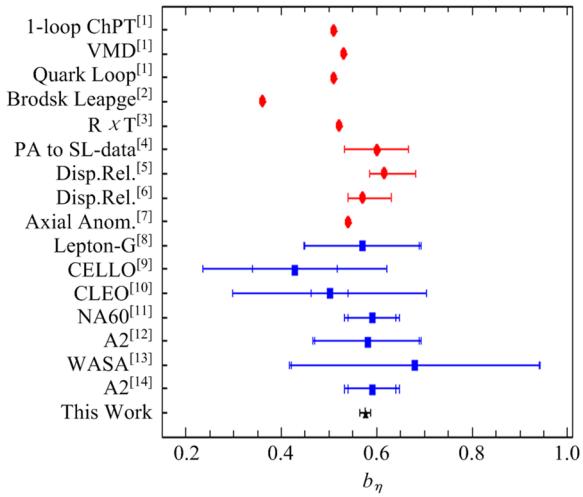

Fig. 3　Slope determinations for η TFF

When comparing different theoretical extractions of the slope of the η TFF with our result in Fig. 3, we find a pretty good agreement with the exception of the results in Ref. [2] that reported $b_\eta = 0.546(9)$ and $b_\eta = 0.521(2)$ using Resonance Chiral theory with one- or two-octet ansätze. The disagreement is between 2 and 5 standard deviations. Ref. [2] uses Resonance Chiral theory, which is based in large-N_c arguments, to extract LEPs. Going from large-N_c to $N_c = 3$ imposes a systematic error[31, 39-40]. Since Ref. [2] considered two approximations for fitting the η TFF (with one and two octets), one could consider the difference between them as a way to estimate such error[3, 42]. In such a way, the η TFF slope would read $b_\eta = 0.53(1)$, at 2.5 standard deviation from our result.

Eventually, we want to comment on the effective single-pole mass determination Λ_P from Eq. (2). Using $b_P = m_P^2/\Lambda_P^2$ and the values in Eq. (4), we obtain $\Lambda_\eta = 0.722(7)\ \text{GeV}$ or $\Lambda_\eta^{-2} = 1.919(39)\ \text{GeV}^{-2}$.

The fits shown in Fig. 1 use the experimental value of the two - photon decay width as an experimental datum to be fitted. Such fit could be repeated without including that decay. In such a way, we reach again a $P_1^7(Q^2)$ and a $P_2^2(Q^2)$ as our best PA with the advantage now that the value $F_{\eta\gamma\gamma}(0)$ is a prediction of our fits. We find $F_{\eta\gamma\gamma}(0)|_{\text{fit}} = 0.250$

(38) GeV^{-1} for the $P_1^7(Q^2)$ and $F_{\eta\gamma\gamma}(0)|_{\rm fit}=0.248$ (28) GeV^{-1} for the $P_2^2(Q^2)$, which translates into $\Gamma_{\eta\gamma\gamma}|_{\rm fit}=0.43(13)$ keV and $\Gamma_{\eta\gamma\gamma}|_{\rm fit}=0.42(10)$ keV, respectively. Compared with the experimental value $\Gamma_{\eta\gamma\gamma}|_{\rm exp}=0.516(18)$ keV such predictions are at 0.66 and 0.94 standard deviation each.

2 Reanalysis of η-η' mixing parameters

In this section we briefly summarize the main elements to extract the mixing parameters exclusively from our fits to the form factor data. As was done in Ref. [3], we analyze η-η' mixing using the quark-flavor basis. In this basis, the η and η' decay constants are parametrized as

$$\begin{pmatrix} F_\eta^q & F_\eta^s \\ F_{\eta'}^q & F_{\eta'}^s \end{pmatrix} = \begin{pmatrix} F_q\cos\phi_q & -F_s\sin\phi_s \\ F_q\sin\phi_q & F_s\cos\phi_s \end{pmatrix} \tag{5}$$

where $F_{q,s}$ are the light-quark and strange pseudoscalar decay constants, respectively, and $\phi_{q,s}$ the related mixing angles. Several phenomenological analyses find $\phi_q\simeq\phi_s$, which is also supported by large-N_c ChPT calculations where the difference between these two angles is seen to be proportional to an OZI-rule violating parameter and hence small[43-44].

Within this approximation, the asymptotic limits of the TFFs take the form

$$\left.\begin{aligned} \lim_{Q^2\to\infty} Q^2F_{\eta\gamma^*\gamma}(Q^2) &= 2(\hat{c}_qF_\eta^q+\hat{c}_sF_\eta^s) = \\ & 2(\hat{c}_qF_q\cos\phi-\hat{c}_sF_s\sin\phi) \\ \lim_{Q^2\to\infty} Q^2F_{\eta'\gamma^*\gamma}(Q^2) &= 2(\hat{c}_qF_{\eta'}^q+\hat{c}_sF_{\eta'}^s) = \\ & 2(\hat{c}_qF_q\sin\phi+\hat{c}_sF_s\cos\phi) \end{aligned}\right\} \tag{6}$$

and their normalization at zero

$$\left.\begin{aligned} F_{\eta\gamma\gamma}(0) &= \frac{1}{4\pi^2}\left(\frac{\hat{c}_qF_{\eta'}^s-\hat{c}_sF_{\eta'}^q}{F_{\eta'}^sF_\eta^q-F_{\eta'}^qF_\eta^s}\right) = \\ & \frac{1}{4\pi^2}\left(\frac{\hat{c}_q}{F_q}\cos\phi-\frac{\hat{c}_s}{F_s}\sin\phi\right) \\ F_{\eta'\gamma\gamma}(0) &= \frac{1}{4\pi^2}\left(\frac{\hat{c}_qF_\eta^s-\hat{c}_sF_\eta^q}{F_\eta^qF_{\eta'}^s-F_\eta^sF_{\eta'}^q}\right) = \\ & \frac{1}{4\pi^2}\left(\frac{\hat{c}_q}{F_q}\sin\phi+\frac{\hat{c}_s}{F_s}\cos\phi\right) \end{aligned}\right\} \tag{7}$$

with $\hat{c}_q=5/3$ and $\hat{c}_s=\sqrt{2}/3$.

Experimental information provides $|F_{\eta\gamma\gamma}(0)|_{\rm exp}=0.274$ (5) GeV^{-1} and $|F_{\eta'\gamma\gamma}(0)|_{\rm exp}=0.344$ (6) GeV^{-1} and for the asymptotic value of the η TFF we take the value shown in Eq. (3) with symmetrical errors, $\lim_{Q^2\to\infty} Q^2F_{\eta\gamma^*\gamma}(Q^2)=0.177$ (15) GeV. With these values, the mixing parameters are predicted to be

$$\left.\begin{aligned} F_q/F_\pi &= 1.07(1),\ F_s/F_\pi = 1.39(14) \\ \phi &= 39.3(1.2)^\circ \end{aligned}\right\} \tag{8}$$

with $F_\pi=92.21(14)$ MeV[34]. The uncertainties are dominated by the error from the asymptotic value prediction.

The mixing parameters obtained with our fits are precise enough to be competitive with the standard approaches with the advantage of using much less input information.

3 A prediction for the $VP\gamma$ couplings

In this section, we extend our analysis to the vector-pseudoscalar electromagnetic form factors. In particular, we are interested in the couplings of the radiative decays of lowest-lying vector mesons into η or η', i.e., $V\to(\eta,\eta')\gamma$, and of the radiative decays $\eta'\to V\gamma$, with $V=\rho,\ \omega,\ \phi$.

We follow closely the method presented in Refs. [44-45], and make use of the equations in Appendix A in Ref. [44] to relate the form factors with the mixing angle and the decay constants in the flavor basis. To account for the $\pi-\omega$ mixing we use $\phi_V=3.4^\circ$. The form factors, saturated with the lowest-lying resonance and then assuming vector meson dominance, can be expressed by

$$F_{VP\gamma}(0,0) = \frac{f_V}{m_V}g_{VP\gamma} \tag{9}$$

where $g_{VP\gamma}$ are the couplings we are interested in, and f_V are the leptonic decay constants of the vector mesons and are determined from the experimental decay rates via

$$\Gamma(V\to e^+e^-) = \frac{4\pi}{3}\alpha^2\frac{f_V^2}{m_V}c_V^2 \tag{10}$$

with c_V is an electric charge factor of the quarks that make up the vector, $c_V=(\frac{1}{\sqrt{2}},\frac{\sin\theta_V}{\sqrt{6}},\frac{\cos\theta_V}{\sqrt{6}})$ for $V=\rho,\ \omega,\ \phi$ respectively. Here $\theta_V=\phi_V+\arctan(1/\sqrt{2})$.

Experimentally we find

$$\left.\begin{aligned} f_{\rho^0} &= (221.2 \pm 0.9)\ \text{MeV} \\ f_{\omega} &= (179.9 \pm 3.1)\ \text{MeV} \\ f_{\phi} &= (239.0 \pm 3.8)\ \text{MeV} \end{aligned}\right\} \quad (11)$$

using $\Gamma(\rho \to e^+e^-) = 7.04(6)$ keV, $\Gamma(\omega \to e^+e^-) = 0.60(2)$ keV, and $\Gamma(\phi \to e^+e^-) = 1.27(4)$ keV from Ref. [34].

The couplings in this flavor basis are:

$$\left.\begin{aligned} g_{\rho\eta\gamma} &= \frac{3m_\rho}{4\pi^2 f_{\rho^0}} \frac{\cos\phi}{\sqrt{2}F_q},\ g_{\rho\eta'\gamma} = \frac{3m_\rho}{4\pi^2 f_{\rho^0}} \frac{\sin\phi}{\sqrt{2}F_q} \\ g_{\omega\eta\gamma} &= \frac{m_\omega}{4\pi^2 f_\omega}\left(\cos\phi_V \frac{\cos\phi}{\sqrt{2}F_q} - 2\sin\phi_V \frac{\sin\phi}{\sqrt{2}F_s}\right) \\ g_{\omega\eta'\gamma} &= \frac{m_\omega}{4\pi^2 f_\omega}\left(\cos\phi_V \frac{\sin\phi}{\sqrt{2}F_q} + 2\sin\phi_V \frac{\cos\phi}{\sqrt{2}F_s}\right) \\ g_{\phi\eta\gamma} &= \frac{m_\phi}{4\pi^2 f_\phi}\left(\sin\phi_V \frac{\cos\phi}{\sqrt{2}F_q} + 2\cos\phi_V \frac{\sinsφ}{\sqrt{2}F_s}\right) \\ g_{\phi\eta'\gamma} &= \frac{m_\phi}{4\pi^2 f_\phi}\left(\sin\phi_V \frac{\sin\phi}{\sqrt{2}F_q} - 2\cos\phi_V \frac{\cos\phi}{\sqrt{2}F_s}\right) \end{aligned}\right\} \quad (12)$$

where we have assumed $\phi_q = \phi_s = \phi$. Tab. 1 collects our predictions in its second column. Corrections due to $\phi_q \neq \phi_s$ to these formulae can be found in Appendix A, Eq. (A.5) of Ref. [44].

Tab. 1　Summary of $VP\gamma$ couplings

parameter	prediction	experoment
$g_{\rho\eta\gamma}$	1.50(4)	1.58(5)
$g_{\rho\eta'\gamma}$	1.18(5)	1.32(3)
$g_{\omega\eta\gamma}$	0.57(2)	0.45(2)
$g_{\omega\eta'\gamma}$	0.55(2)	0.43(2)
$g_{\phi\eta\gamma}$	−0.83(11)	−0.69(1)
$g_{\phi\eta'\gamma}$	0.98(14)	0.72(1)
$R_{J/\Psi} = \frac{\Gamma(J/\Psi \to \eta'\gamma)}{\Gamma(J/\Psi \to \eta\gamma)}$	4.74(55)	4.67(20)

The decay widths of $P \to V\gamma$ and $V \to P\gamma$ are

$$\left.\begin{aligned} \Gamma(P \to V\gamma) &= \frac{\alpha}{8} g^2_{VP\gamma}\left(\frac{m_P^2 - m_V^2}{m_P}\right) \\ \Gamma(V \to P\gamma) &= \frac{\alpha}{24} g^2_{VP\gamma}\left(\frac{m_V^2 - m_P^2}{m_V}\right) \end{aligned}\right\} \quad (13)$$

The experimental decay widths from Ref. [34] allow us to extract an experimental value for $g_{VP\gamma}$, which are collected in the last column in Tab. 1, experimental determinations are from Ref. [34].

Our predictions compare well with the experimental determinations, see Tab. 1, specially considering the simplicity of the approach. The differences are always below 2 standard deviations, excepting the ω couplings. Our prediction for the ratio of J/Ψ decays is in that respect remarkable.

4　Conclusion

In the present work, the η transition form factor has been analyzed for the first time in both space- and time-like regions at low and intermediate energies, making use of a model-independent approach based on the use of rational approximants of Padé type. The model independence of our approach is achieved trough a detailed and conservative evaluation of the systematic error associated with it. The new set of experimental data on the $\eta \to e^+e^-\gamma$ reaction provided by the A2 Collaboration in the very low-energy part of the time-like region allows for a much better determination of the slope and curvature parameters of the form factor, as compared to the predictions obtained in our previous work only using space-like data, which constitute the most precise values up-to-date of these low-energy parameters. Our method is also able to predict for the first time the third derivative of the form factor. In addition, the new analysis has served to further constrain its values at zero momentum transfer and infinity. We have seen that our results, in particular for the case of the slope parameter, are quite insensitive to the values used in the fits for the two-photon decay width of the η, thus showing that the collection of space- and time-like experimental data is more than enough to fix a value for the normalization of the form factor compatible with current measurements. We have also seen that the role played by the high-energy space-like data is crucial to getting accurate predictions for the low-energy parameters of the form factor and its asymptotic value. As a consequence of these new results, we have fully reanalyzed the η-η' mixing parameters this time also considering renormalisation-scale dependent effects of the singlet decay constant F_0. The new values obtained are

already competitive with standard results with the advantage of requiring much less input information. Related to this, we have also obtained predictions for the $VP\gamma$ couplings which are in the ballpark of present-day determinations.

In summary, the method of Padé approximants has been shown to be very powerful for fixing the low-energy properties of the η transition form factor, making their predictions more accurate and well-established. This fact opens the door to a more exhaustive analysis of the single Dalitz decay processes $P\to l^+ l^- \gamma$, with $P=\pi^0$, η, η' and $l=e$, μ, the double Dalitz ones $P\to l^+ l^- l^+ l^-$ (in all possible kinematically allowed configurations)[46], and the rare lepton-pair decays $P\to l^+ l^-$ (see the $\pi^0\to e^+ e^-$ application in Ref. [47]), which are usually discussed only in terms of monopole approximations. Indeed, when this work was being concluded the BES Ⅲ Collaboration reported a first observation of the $\eta'\to ze^+e^-\gamma$ process measuring the branching ratio and extracting the η' transition form factor[48]. This new measurement may put our approach with its back to the wall. However, a very preliminary analysis of this recent data in comparison with our prediction for this form factor in the time-like region exhibits a nice agreement but reveals the necessity of going beyond the vector meson dominance model used in the experimental analysis[49].

References

[1] AMETLLER L, BIJNENS J, BRAMON A, et al. Transition form factors in π^0, η, and η' couplings to $\gamma\gamma^*$ [J]. Physical Review D, 1992, 45(3): 986-989.

[2] CZYŽH, IVASHYN S, KORCHIN A, et al. Two-photon form factors of the π^0, η, and η' mesons in the chiral theory with resonances[J]. Physical Review D, 2012, 85(9): 094010(1-11).

[3] ESCRIBANOR, MASJUAN P, SANCHEZ-PUERTAS P. η, and η' transition form factors from rational approximants[J]. Physical Review D, 2014, 89(3): 034014(1-15).

[4] HANHART C, KUPSC A, MEISSNER U G, ET AL. Dispersive analysis for $\eta\to\gamma\gamma^*$ [J]. European Physical Journal C, 2013, 73(12): 2668(1-11).

[5] KLOPOT Y, OGANESIAN A, TERYAEV O. Axial anomaly and vector meson dominance model[J]. JETP Letters, 2014, 99(12): 679-684.

[6] DJHELYADINR I, GOLOVKIN S V, KACHANOV V A, et al. Investigation of the electromagnetic structure of the η meson in the decay $\eta\to\mu^+\mu^-\gamma$[J]. Physics Letters B, 1980, 94(4): 548-550.

[7] BEHREND H J, CRIEGEE L, FIELD J H, et al. A measurement of the π^0, η, and η' electromagnetic form factors[J]. Zeitschrift Für Physik C, 1991, 49(3): 401-409.

[8] GRONBERG J, HILL T S, KUTSCHKE R, et al. Measurements of the meson-photon transition form factors of light pseudoscalar mesons at large momentum transfer [J]. Physical Review D, 1998, 57(1): 33-54.

[9] ARNALDI R, BANICZ K, CASTON J, et al. Study of the electromagnetic transition form-factors in $\mu^+\mu^-\gamma$ and $\omega\to\mu^+\mu^-\pi^0$ decays with NA60[J]. Physics Letters B, 2009, 677(5): 260-266.

[10] BERGHÄUSER H, METAG V, STAROSTIN A, et al. Determination of the η-transition form factor in the $\gamma p\to p\eta\to p\gamma e^+e^-$ reaction[J]. Physics Letters B, 2011, 701(5): 562-567.

[11] HODANAM, MOSKAL P. Study of the $\eta\to e^+e^-\gamma$ decay using WASA-at-COSY detector system[C]// EPJ Web Conference. EDP Sciences, 2012, 37: 09017.

[12] AGUAR-BARTOLOMÉP, ANNAND P, ARENDS J R M, et al. New determination of the η transition form factor in the Dalitz decay $\eta\to e^+e^-\gamma$ with the Crystal Ball/TAPS detectors at the Mainz Microtron[J]. Physical Review C, 2014, 89(4): 044608.

[13] KROLL P. The form factors for the photon to pseudoscalar meson transitions - an update[J]. European Physics Journal C, 2011, 71: 1623(1-33).

[14] DOROKHOV A E, RADZHABOV A E, ZHEVLAKOV A S. The pseudoscalar hadronic channel contribution of the light-by-light process to the muon $(g-2)$ μ within the nonlocal chiral quark model [J]. European Physics Journal C, 2011, 71(7): 1702(1-12).

[15] BRODSKY S J, CAO F G, DE TERAMOND G F. Evolved QCD predictions for the meson-photon transition form factors[J]. Physical Review D, 2011, 84(3): 033001(1-34).

[16] BRODSKY S J, CAO F G, DE TERAMOND G F. Meson transition form factors in light-front holographic QCD[J]. Physical Review D, 2011, 84(7): 2437-2452.

[17] KLOPOTY N, OGANESIAN A G, TERYAEV O V. Axial anomaly and mixing: from real to highly virtual photons [J]. Physical Review D, 2011, 84(5): 412-419.

[18] WU X G, HUANG T. Constraints on the light pseudoscalar meson distribution amplitudes from their meson-photon transition form factors[J]. Physical Review D, 2011, 84(7): 443-444.

[19] NOGUERA S, SCOPETTA S. The eta-photon transition

form factor[J]. Physical Review D, 2012, 85: 054004.

[20] BALAKIREVA I, LUCHA W, MELIKHOV D. Pion elastic and $(\pi 0, \eta, \eta') \to \gamma\gamma^*$ transition form factors in a broad range of momentum transfers [J]. Physical Review D, 2012, 85(2012) 036006(1-7).

[21] MELIKHOV D, STECH B. On the $\gamma^* \gamma \to \pi(\eta, \eta')$ transition form factors [J]. Physical Review D, 2012, (5): 051901(1-4).

[22] KROLL P, PASSEK-KUMERICKI K. The $\eta(\eta')$ gamma transition form factor and the gluon-gluon distribution amplitude [J]. Journal of Physics G, 2012, 40(7): 75005-75021.

[23] MELIKHOV D, STECH B. Universal behavior of the $\gamma^* \gamma \to (\pi^0, \eta, \eta')$ transition form factors [J]. Physics Letters B, 2012, 718(2): 488-491.

[24] GENG C Q, Lih C C. Erratum: Pseudoscalar transition form factors within the light-front quark model [J]. Physical Review C, 2013, 87(3): 039901.

[25] KLOPOT Y, OGANESIAN A, TERYAEV O. Transition form factors and mixing of pseudoscalar mesons from anomaly sum rule [J]. Physical Review D, 2013, 87: 036013.

[26] BIJNENS J, BRAMON A, CORNET F. Pseudoscalar decays into two photons in chiral perturbation theory[J]. Physical Review Letters, 1988, 61(113): 1453-1456.

[27] BIJNENS J, BRAMON A, CORNET F. Chiral perturbation theory for anomalous processes [J]. Zeitschrift Für Physik C, 1990, 46(4): 599-607.

[28] MASJUAN P. $\gamma^* \gamma \to \pi^0$ transition form factor at low-energies from a model-independent approach [J]. Physical Review D, 2012, 86: 094021(1-9).

[29] BAKERG A, GRAVES-MORRIS P. Padé Approximants, Encyclopedia of Mathematics and its Applications [M]. Cambridge University Press, 1996.

[30] MASJUAN P, PERIS S, SANZ-CILLERO J J. Vector meson dominance as a first step in a systematic approximation: The pion vector form factor[J]. Physical Review D, 2008, 78(7): 074028(1-12).

[31] MASJUAN P. Rational approximations in quantum chromodynamics [J]. Eprint Arxiv, 2010: arXiv: 1005.5683.

[32] LEPAGE G P, Brodsky S J. Exclusive processes in quantum chromodynamics: Evolution equations for hadronic wavefunctions and the form factors of mesons [J]. Physical Review D, 1980, 22: 2157.

[33] DEL AMO SANCHEZ P, LEES J P, POIREAU V, et al. Measurement of the $\gamma\gamma^* \to \eta$ and $\gamma\gamma^* \to \eta'$ transition form factors [J]. Physical Review D, 2011, 84(38): 1821-1824.

[34] OLIVE K A, AGASHE A, AMSLER C, et al. Review of particle physics [J]. Chinese Physics C, 2014, 38: 090001.

[35] BABUSCI D, BADONI D, BALWIERZ-PYTKO I, et al. Measurement of η meson production in $\gamma\gamma$ interactions and $\Gamma(\eta \to \gamma\gamma)$ with the KLOE detector[J]. Journal of High Energy Physics, 2013, 119(1): 1301(1-23).

[36] AUBERT B, BARATE M, BONA D, et al. Measurement of the η and η' transition form factors at $q^2 = 112$ GeV^2 [J]. Physical Review D, 2006, 74(1): 012002(1-14).

[37] BRODSKY S J, LEPAGE G P. Large-angle two-photon exclusive channels in quantum chromodynamics [J]. Physical Review D, 1981, 24(7): 1808-1817.

[38] KUBIS B, PLENTER J. Anomalous decay and scattering processes of the eta meson[J]. European Physical Journal C, 2015, 75(6): 1-12.

[39] MASJUAN P, PERIS S. A rational approach to resonance saturation in large-N_c QCD [J]. Journal of High Energy Physics, 2007, (5): 1285-1291.

[40] MASJUAN P, PERIS S. A rational approximation to $<VV-AA>$ and its $\mathcal{O}(p^6)$ low-energy constant [J]. Physics Letters B, 2008, 663(1): 61-65.

[41] MASJUAN P, ARRIOLA E R, BRONIOWSKI W. Meson dominance of hadron form factors and large-N_c phenomenology[J]. Physical Review D, 2013, 87(1): 014005(1-16).

[42] MASJUAN P, VANDERHAEGHEN M. Ballpark prediction for the hadronic light-by-light contribution to the muon $(g-2)_\mu$ [J]. Journal of Physics G, 2015, 42(12): 10-12.

[43] FELDMANN T, KROLL P, STECH B. Mixing and decay constants of pseudoscalar mesons [J]. Physical Review D, 1998, 58(11): 398-399.

[44] ESCRIBANOR, FRÈRE J M. Study of the η-η' system in the two mixing angle scheme[J]. Journal of High Energy Physics, 2005, (6): arXiv:hep-ph/0501072.

[45] BALL P, FRÈRE J M, TYTGAT M. Phenomenological evidence for the gluon content of η and η' [J]. Physics Letters B, 1996, 365(1-4): 367376.

[46] ESCRIBANO R, GONZÀLEZ-SOLÍSR S. A data-driven model-independent approach to π^0, η and η' single and double Dalitz decays[J]. 2015: arXiv:1511.04916.

[47] MASJUAN P, SANCHEZ-PUERTAS P. Phenomenology of bivariate approximants: The $\pi^0 \to e^+ e^-$ case and its impact on the electron and muon g-2 [J]. Blood, 2015, 98(10): 3169-3171.

[48] ABLIKIM M, ACHASOV M N, AI X C, et al. Observation of the Dalitz decay $\eta' \to \gamma e^+ e^-$ [J]. Physical Review D, 2015, 92: 012001(1-11).

[49] ESCRIBANO R, GONZÀLEZ-SOÍLSR S, MASJUAN P, et al. The η' transition form factor from space- and time-like experimental data [J]. European Physical Journal C, 2015, 75(9): 1-16.